Interaction of longitudinal-optic phonons with free holes as evidenced in Raman spectra from Be-doped *p*-type GaAs

Kam Wan and Jeff F. Young
Division of Physics, National Research Council, Ottawa, Canada K1A 0R6
(Received 20 October 1989)

The interaction between small-wave-vector, longitudinal-optic (LO) lattice vibrations and free-hole plasmas in Be-doped *p*-type GaAs is studied with use of nonresonant, allowed Raman scattering. In contrast to the coupled LO-phonon–plasmon modes, ω_+ and ω_- typically observed in *n*-type zinc-blende-structure semiconductors, only one mode is observed for hole densities between 1×10^{18} and 1.6×10^{19} cm^{-3}. With increasing hole density, this single mode shifts first to higher energies, then back to lower energies, between that of the LO and transverse-optic (TO) phonons, and finally asymptotes at the TO-phonon energy. The observed Raman spectra are accurately fitted with calculated coupled-mode spectra which take into account wave-vector-dependent intra- and inter-valence-band transitions within the heavy- and light-hole bands. Intra-light-hole and inter-heavy- to light-hole transitions are shown to make very significant contributions to the spectra, although they alone cannot account for the novel density dependence of the coupled-mode energy. A detailed analysis of the coupled-mode dependence on wave vector and phenomenological damping reveals that the observed density dependence can, in principle, occur even in a single-component plasma due to two distinctly different physical mechanisms. In the case of the *p*-type GaAs studied here, it is shown that the novel density dependence is primarily due to the overdamped nature of intra-heavy-hole transitions.

I. INTRODUCTION

Following the first discussion of coupled plasmon-phonon modes by Varga,[1] the interaction between free-carrier plasmas and longitudinal-optic (LO) phonons in zinc-blende-structure semiconductors has been studied extensively both from experimental and theoretical viewpoints.[2–4] The vast majority of this work has dealt with free-electron plasmas in *n*-type semiconductors. In these materials, the coupling between the LO phonon and the free-carrier plasma usually yields two modes, referred to as coupled plasmon–LO-phonon modes (CPPM's), ω_+ and ω_-. The coupling occurs via the macroscopic electric fields associated with both of these excitations. The degree of coupling, or mixing, is largest when their energies are comparable. Although the precise density dependence of the energies of the CPPM's is influenced by wave-vector dispersion,[4] nonparabolic band structure,[5] and damping processes,[6] the same general behavior as schematically shown by the solid lines in Fig. 1 has been observed in a variety of semiconductors. Two nonintersecting branches are formed. The high-energy, ω_+ branch starts with the LO-phonon energy at low densities. With increasing density, its energy monotonically increases and asymptotically assumes the energy of a pure plasmon. The low-energy, ω_- branch behaves like a pure plasmon for low densities, increases its energy monotonically with density, and asymptotes at the transverse-optic (TO) phonon energy at high densities.

Relatively little work has been reported on the interaction of free-hole plasmas with LO phonons. Olego and Cardona[7] have observed a hole-density dependence of the LO-phonon line in Zn-doped *p*-type GaAs samples using resonant Raman scattering in a polarized scattering geometry. They interpreted their results in terms of large wave-vector phonon scattering induced by impurities. Kamijoh *et al.*[8] have observed a LO-phonon peak using a depolarized scattering geometry in Si-doped GaAs samples grown by liquid-phase epitaxy. It exhibited an increasing linewidth, but stationary peak energy for hole

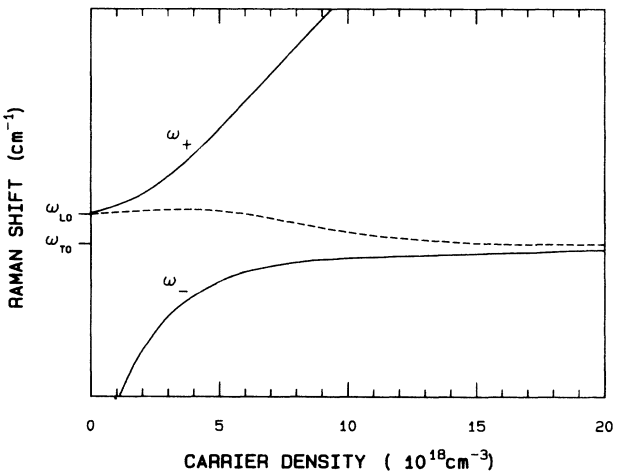

FIG. 1. A schematic illustration of the difference between the carrier-density-dependent energies of the two-coupled plasmon–LO-phonon modes typically observed in *n*-type semiconductors (solid) and the density-dependent energy of the single-mode peak observed in the Raman spectra from Be-doped *p*-type GaAs (dots).

concentrations ranging from 10^{17} to 5×10^{18} cm^{-3}. They interpreted their results using expressions similar to those of Olego and Cardona. Recently, Yuasa and Ishii[9] reported observing CPPM's in their Raman studies of Be-doped p-type GaAs grown by molecular-beam epitaxy (MBE). They qualitatively concluded that the CPPM's in p-type GaAs behave similarly to those normally observed in n-type materials.

In this paper we present Raman spectra from a series of Be-doped, p-type GaAs samples grown by MBE, obtained using a depolarized, allowed scattering geometry. These spectra clearly reveal the different nature of the plasma–LO-phonon coupling in p-type GaAs as compared to that previously observed in n-type semiconductors. In particular, for hole densities in the range of 3×10^{18} to 6×10^{18} cm^{-3}, only a single peak is observed with a density-dependent energy between the LO- and TO-phonon values. This unusual behavior is schematically represented by the dashed curve in Fig. 1.

Following the presentation of these results in Sec. II, Sec. III describes how the standard theory for calculating coupled-mode Raman spectra in n-type zinc-blende-structure semiconductors can be modified to include the degenerate, spin-$\frac{3}{2}$-like heavy- and light-hole valence bands. The ability of this modified theory to successfully fit the p-type spectra at a number of different densities strongly suggests that these Raman spectra do in fact represent a direct measure of the free-hole plasma–LO-phonon interaction at relatively small wave vectors. In addition to providing a practical means of optically determining free-hole concentrations in p-type GaAs, this also allows us to probe further into the nature of this spin-$\frac{3}{2}$ plasma–LO-phonon interaction.

In Sec. IV, the very significant contributions of both intra-light-hole and inter-heavy to light-hole transitions to the overall line shapes and to the density dependence of the peak energy are demonstrated. However, it is also shown that these intrinsic effects associated with the multicomponent nature of the plasma do not, by themselves, account for the novel single-mode behavior of the CPPM's observed. In fact, if only the intra-heavy-hole term is retained in the calculation, the resulting behavior is even more strongly (in a sense to be defined below) single-mode-like.

Section V contains a detailed analysis of physical mechanisms that can in principle lead to the novel density dependence of the CPPM's reported here. It is shown that such a density dependence can in general be caused by dispersion-related effects at large wave vectors, and by damping-related effects independent of wave vector. Two limiting cases in which each of these effects acts independently are discussed; the first involves large wave-vector modes with no phenomenological damping present and the second involves strong phenomenological damping in the limit of zero wave vector. The single-mode behavior observed in p-type GaAs is shown to be largely due to the overdamped nature of intra-heavy-hole transitions in this system.

II. EXPERIMENT AND RESULTS

The Raman spectra presented in this paper were obtained using a standard backscattering configuration from a (100) surface of Be-doped, MBE-grown p-type GaAs samples. Thick (>1-μm) epitaxial layers were grown on semi-insulating GaAs substrates. The hole concentrations and mobilities of the samples as determined from room-temperature Hall measurements are listed in Table I. The Raman excitation source was a frequency-doubled yttrium aluminum garnet (YAG) laser at 532 nm with an average power of 250 mW. The skin depth of the 532-nm radiation in GaAs is about 0.1 μm, which is much thinner than the epilayer. The finite absorption depth leads to an uncertainty of 0.8×10^{5} cm^{-1} in wave vector, which, as is shown later, has a negligible effect on our interpretation of our spectra. The beam was polarized in the [010] direction and its intensity on the sample surface was adjusted to ensure that optically injected carriers did not contribute to the spectra. The backscattered light, polarized parallel to the [001] direction, was analyzed with a SPEX Industries Triplemate spectrograph. A Si charge-coupled array detector was used to record the spectra. The spectral resolution was <5 cm^{-1}.

Room-temperature Raman spectra obtained from the five samples described in Table I are shown as dots in Fig. 2. The spectra generally consist of a sharp peak at 291 cm^{-1}, superimposed on a broader, asymmetric line with a tail extending to high energy. The sharp feature at 291 cm^{-1} is due to scattering from the unscreened LO phonons in the depletion region near the sample surface, as evidenced by its energy and its decreasing strength at larger carrier densities. The broader peak is associated with the interaction of the free holes and LO phonons in the bulk of the epilayer. The peak position of the broad structure starts at the LO-phonon energy (291 cm^{-1}) in sample (a), shifts to a slightly higher energy in sample (b), then decreases below the LO-phonon energy, but above

TABLE I. Sample characteristics.

Sample	Hall measurements		Raman measurements
	total hole density (10^{18} cm^{-3})	Mobility (cm^2/V s)	Total hole density (10^{18} cm^{-3})
(a)	1.0	175.0	1.1
(b)	4.5	123.0	2.25
(c)	6.0	100.0	3.6
(d)	8.0	120.0	5.25
(e)	30.0		16.0

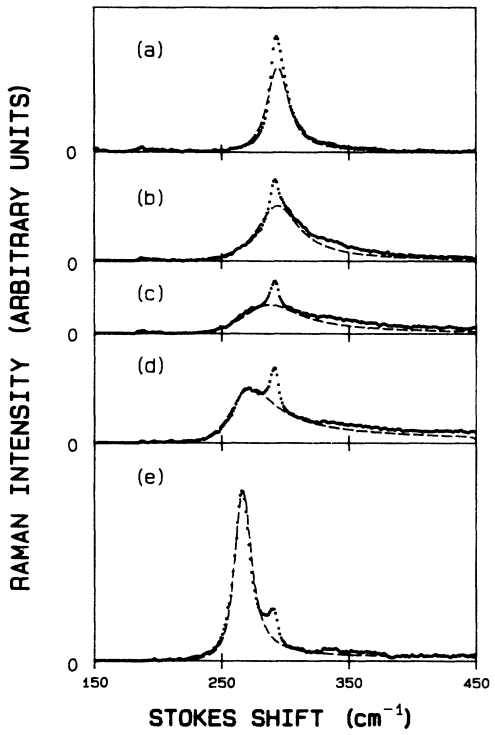

FIG. 2. The measured (dots) and calculated (dashes) Raman spectra from the five Be-doped p-type GaAs samples described in Table I.

the TO-phonon energy in samples (c) and (d), and finally goes to just below the TO-phonon energy in sample (e). This concentration dependence of CPPM's is clearly different from that normally observed in n-type semiconductors, and, to our knowledge, has not been previously observed in any material.

It is essential to emphasize that these spectra were obtained in a depolarized scattering geometry from a (100)-oriented surface where zone center LO-phonon scattering is allowed. [TO-phonon scattering is always forbidden from (100) surface.] Figure 3 compares the spectra from sample (d) in the two scattering polarizations. The coupling-related, broad peak dominates the ($\perp$,$\parallel$) spectrum (solid), but is absent in the ($\parallel$,$\parallel$) spectrum (dashed). The weak, sharp peak at about 268 cm^{-1} is due to forbidden TO-phonon scattering. A similar polarization dependence was obtained from the other four samples. Two conclusions can be drawn from this comparison. First, it is clearly shown that the nature of the coupled mode in our samples is different from that reported by Olego and Cardona.[7] The mode we observe has the symmetry of the zone-center LO phonon, while the mode they observe does not. According to their interpretation, the forbidden mode they measured consists of LO phonons with a range of large wave vectors. These phonons are made visible by symmetry breaking due to impurity potentials. From the viewpoint of material characterization, the above comparison suggests that the potential fluctuations induced by Be in MBE-grown samples are much less than those associated with Zn in bulk samples. Second, it has been suggested[10] that in backscattering from opaque materials, the uncertainty in the scattering wave vector associated with the finite skin depth should be considered in the interpretation of the spectra. The absence of the forbidden peak in our ($\parallel$,$\parallel$) spectra indicates that large wave-vector, nonallowed scattering is weak in our system, and therefore it is safe to neglect the absorption-related wave-vector uncertainty in our line-shape calculations.

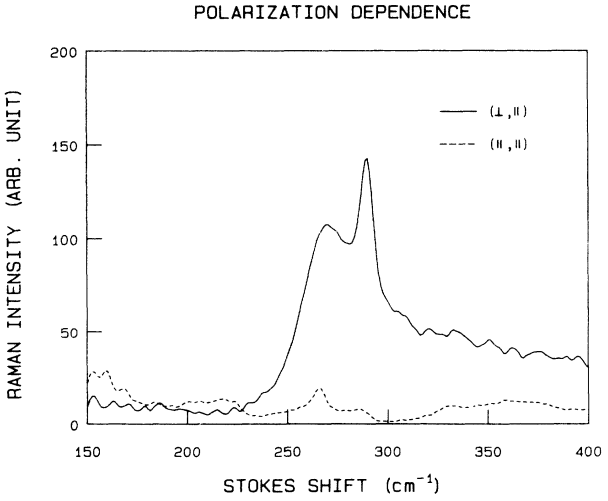

FIG. 3. The Raman spectra from sample (d) in ($\perp$,$\parallel$) (solid) and ($\parallel$,$\parallel$) (dashed) scattering polarizations.

While the difference between our Raman spectra and those of Olego and Cardona[7] might be mainly due to differences in sample growth and doping, the sample quality used by Yuasa and Ishii[9] should be very similar to ours. They did not observe the novel hole-density dependence of the coupled mode because of the hole densities of their samples. Comparing our Raman spectra (Fig. 2) with theirs (Fig. 1 of their paper), their spectra correspond to our (a), (b), and (e). They did not measure the most critical spectra (c) and (d). Without these two spectra, they concluded that the coupled modes in p-type GaAs behave as those usually observed in n-type semiconductors.

III. CALCULATION OF RAMAN LINE SHAPES

To support the assignment of the broad asymmetric peak to CPPM's, the Raman cross sections were calculated and shown as dashed lines in Fig. 2. This calculation employs a theory similar, but not identical, to those developed by Hon and Faust[6] and Klein *et al.*[11] independently for Raman line-shape analysis in n-type semiconductors. For depolarized scattering geometry, where scattering is due to electro-optic and deformation-potential mechanisms, the results from these two papers are the same. Following Hon and Faust,[6] the differential Raman cross section can be expressed as

$$\frac{d^2R}{d\omega\, d\Omega} \propto \mathrm{Im}\left\{\frac{-\epsilon_\infty}{\epsilon}\left[\frac{-\epsilon_\infty}{4\pi}+2CA\chi_I - C^2A^2\chi_I\left[1+\frac{4\pi}{\epsilon_\infty}\chi_{\mathrm{fc}}\right]\right]\right\}, \quad (1)$$

where

$$\epsilon=\epsilon_\infty+4\pi(\chi_I+\chi_{\rm fc}) , \tag{2}$$

$$A=\frac{\omega_t^2}{\omega_l^2-\omega_t^2} , \tag{3}$$

and

$$4\pi\chi_I=\frac{\omega_l^2-\omega_t^2}{\omega_t^2-\omega^2-i\Gamma_I\omega} . \tag{4}$$

Here ϵ is the total dielectric function of the system, $C=-0.59$ is the Faust-Henry coefficient for GaAs, and ω_l and ω_t are the unscreened, Brillouin-zone-center LO-phonon (291 cm^{-1}) and TO-phonon (268 cm^{-1}) energies, respectively. χ_I is the ionic susceptibility of the zinc-blende structure, and $\chi_{\rm fc}$ is the susceptibility of the free carriers. For n-type material, the wave vector (q) and frequency (ω) dependent free-carrier susceptibility derives from intra-conduction-band transitions, and is taken to be of the Lindhard-Mermin[12] form, generalized to nonzero temperatures and Maxwell-Boltzmann distributions. Then

$$\chi_{\rm fc}(q,\omega)\frac{(1+i\Gamma_{\rm fc}/\omega)\chi^0_{\rm fc}(q,\omega)}{1+i\Gamma_{\rm fc}\chi^0_{\rm fc}(q,\omega)/\omega\chi^0_{\rm fc}(q,0)} \tag{5}$$

with

$$\chi^0_{\rm fc}(q,\omega)=\frac{\epsilon_\infty}{4\pi}\frac{1+\eta Z(\eta)}{\lambda_D^2 q^2} , \tag{6}$$

where

$$\eta=\left[\frac{m^*_{\rm fc}}{2k_BT}\right]^{1/2}\frac{(\omega+i\Gamma_{\rm fc})}{q} \tag{7}$$

and

$$\lambda_D^2=\frac{\epsilon_\infty k_BT}{4\pi N_{\rm fc}e^2} . \tag{8}$$

Here $N_{\rm fc}$ and $m^*_{\rm fc}$ are the concentration and effective mass of the free carriers, k_BT is Boltzmann's temperature factor, and e is the electronic charge. $\Gamma_{\rm fc}$ is a phenomenological damping constant associated with extrinsic interactions of the free carriers with phonons and impurities, and $Z(\eta)$ is the plasma-dispersion function. To calculate the spectra from p-type GaAs, considering only the heavy- and light-hole bands, $\chi_{\rm fc}$ was approximated by

$$\chi_{\rm fc}=\chi_{\rm lh}+\chi_{\rm hh}+\chi_{\rm inter} , \tag{9}$$

where $\chi_{\rm hh}$ and $\chi_{\rm lh}$ correspond to intra-heavy-hole and intra-light-hole band transitions, which are of the same form as Eq. (5), with the appropriate mass and density parameters. The $\chi_{\rm inter}$ corresponds to inter-valence-band transitions and was obtained by generalizing Bardyszewski's[13] expression of $\chi_{\rm inter}$ at $T=0$ K to finite temperature, in the limit of zero wave vector. Then

$$\mathrm{Im}[\chi_{\rm inter}(\omega)]=\frac{1}{4\pi}\frac{2e^4m^*_{\rm hh}m^*_{\rm lh}}{\omega\hbar^3(m^*_{\rm hh}-m^*_{\rm lh})}[f_{\rm hh}(K)-f_{\rm lh}(K)] , \tag{10}$$

where the $f_{\rm lh}(K)$ and $f_{\rm hh}(K)$ are the Maxwell-Boltzmann distribution functions evaluated at wave vector K, and

$$K^2=\frac{2\omega m^*_{\rm lh}m^*_{\rm hh}}{\hbar(m^*_{\rm hh}-m^*_{\rm lh})} . \tag{11}$$

The real part of $\chi_{\rm inter}$ was obtained numerically using Eq. (10) and the Kramers-Kronig relation. In equilibrium, the light-hole and heavy-hole densities are related as $N_{\rm hh}/N_{\rm lh}=(m^*_{\rm hh}/m^*_{\rm lh})^{3/2}$, hence there are only three variable parameters in the model described by Eqs. (1)–(11); the total hole density and the phenomenological damping parameters for the intraband susceptibilities $\Gamma_{\rm hh}$ and $\Gamma_{\rm lh}$. A self-consistent treatment of phenomenological damping in the interband susceptibility term[14] remains to be incorporated in the model. To reduce the number of independent parameters further, the phenomenological damping terms were weighted in proportion to the respective carrier masses as $\Gamma_{\rm hh}/\Gamma_{\rm lh}=(m^*_{\rm hh}/m^*_{\rm lh})^{3/2}$. The power of $\frac{3}{2}$ provided similar quality fits to all of the observed spectra, for a fixed value of $\Gamma_{\rm lh}=50$ cm^{-1}. These fits, shown superimposed on the experimental data as dashed lines in Fig. 2, were obtained using the densities listed in the last column of Table I,[15] along with the material constants listed in Table II. The discrepancy between the densities extracted using the Raman spectra and those obtained from Hall measurements (also shown in Table I) could be due to the fact that the effective Hall coefficient was taken as unity, whereas due to the complex valence-band structure this coefficient is likely different from unity, as explained in Ref. 17.

The quality of the fits is considered good, with the

TABLE II. List of parameters used in calculations

Symbol	Description	Value
$m^*_{\rm lh}$	Light-hole effective mass	$0.082m_0$
$m^*_{\rm hh}$	Heavy-hole effective mass	$0.45m_0$
C	Faust-Henry coefficient	-0.59
Γ_I	Ionic damping constant	3 cm^{-1}
T	Temperature	300 K
ϵ_∞	High-frequency dielectric constant	10.92
ω_t	TO-phonon energy	268.0 cm^{-1}
ω_l	LO-phonon energy	291.0 cm^{-1}

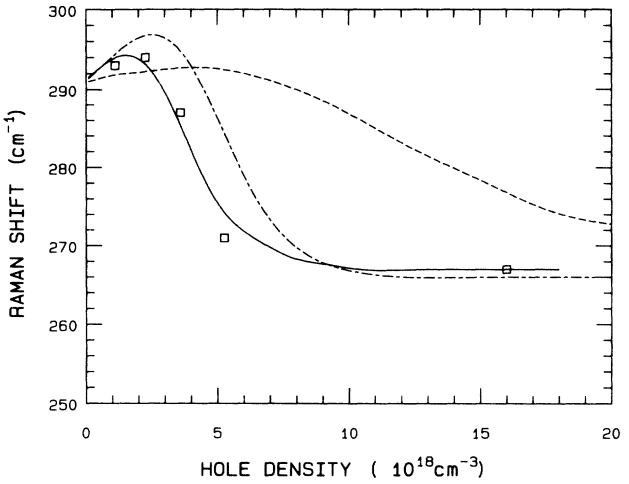

FIG. 4. The measured energies of the peak in the coupled-mode Raman spectra shown in Fig. 2 (squares). The solid curves correspond to peak energies calculated with $\chi_{fc}=\chi_{hh}+\chi_{lh}+\chi_{lh}+\chi_{inter}$ (solid), $\chi_{fc}=\chi_{hh}+\chi_{lh}$ (dashed-dotted), and $\chi_{fc}=\chi_{hh}$ (dots).

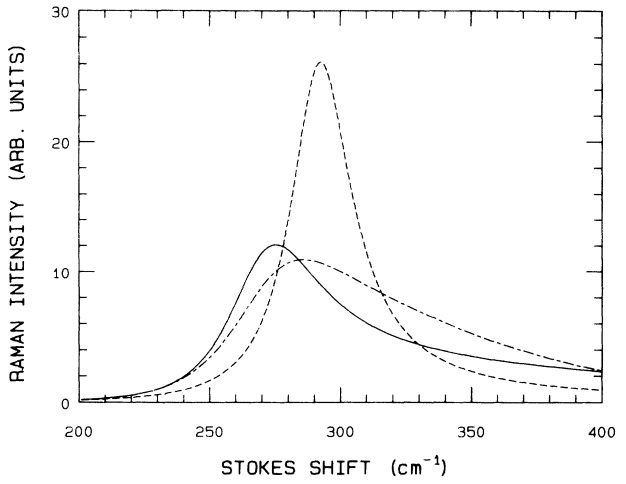

FIG. 5. Spectra calculated for hole density 5.25×10^{18} cm^{-3} using Eq. (1) with $\chi_{fc}=\chi_{hh}+\chi_{lh}+\chi_{inter}$ (solid), $\chi_{fc}=\chi_{hh}+\chi_{lh}$ (dashed-dotted), and $\chi_{fc}=\chi_{hh}$ (dots).

main discrepancy being in the high-energy tail. Better agreement in this range might be obtained if phenomenological damping was included in the interband susceptibility term. Some, but not all of the difference could also be accounted for by errors made in subtracting off a small, broad background from the measured spectra. Regardless of these minor discrepancies, the model exhibits the novel, hole-density dependence of the single mode. This point is emphasized by plotting the observed (squares) and calculated (solid line) peak positions of the CPPM's as a function of hole density in Fig. 4. Although previous Raman line-shape calculations[6,18] have suggested the possibility that coupled modes could have energies between that of the TO- and LO-phonons even at small wave vectors, this aspect of coupled-mode behavior has not been explored in detail.

IV. CONTRIBUTIONS DUE TO INTRA-LIGHT-HOLE AND INTER-VALENCE-BAND TRANSITIONS

Having demonstrated that the novel single-mode spectra observed in Be-doped p-type GaAs can be quantitatively described by a detailed calculation for allowed Raman scattering from a degenerate, two-band, spin-$\frac{3}{2}$ free-carrier system including phenomenological damping, it remains to elucidate the relative importance of intrinsic, spin-$\frac{3}{2}$ related effects, and extrinsic effects related to the phononmenological damping. Although others have incorporated interband transitions in their calculated spectra,[19,20] to our knowledge the relative importance of these various contributions has never been discussed in detail.

The importance of including intra-light-hole transitions, despite the fact that less than 10% of the total hole population is in the light-hole-band and inter-valence-band transitions in the calculation of the spectra is illustrated in Fig. 5. This figure shows the calculated spectra corresponding to sample (d) for which only intra-heavy-hole transitions (dashed), intra-heavy and intra-light-hole transitions (dashed-dotted), and all intraband and interband transitions (solid) are included. The influences of the light holes and the interband transitions are indeed strong.

To demonstrate the influence of inter-valence-band transitions on the density dependence of the CPPM's peaks, the carrier density-dependent coupled-mode energy calculated with the χ_{inter} term omitted from χ_{fc} is shown as a dashed-dotted line in Fig. 4. This may be compared with the dashed line that represents the same calculation but with omission of both χ_{inter} and χ_{lh} from χ_{fc}, and with the full calculation shown as a solid line in Fig. 4. Notice the trend; without the interband term present, the relatively weakly damped (recall the phenomenological damping parameter varies as $m^{3/2}$) light holes, together with the relatively strongly damped heavy holes still yield a single-mode-like system. However it is just on the verge of converting to the more commonly observed two-mode system, which occurs when the slope of the curves in Fig. 4 goes positive in the transition region. Addition of the inter-valence-band term makes the system more single-mode like, while inclusion of only the heavy holes yields a strongly single-mode-like system. This implies that although the inter-valence-band and intra-light-hole transitions strongly influence the quantitative details of the single-mode behavior, the basic source of this behavior can be attributed to the intra-heavy-hole transitions alone.

V. PHYSICAL MECHANISMS RESPONSIBLE FOR SINGLE-MODE BEHAVIOR

Since the single-mode behavior in the p-type GaAs has been traced to the intra-heavy-hole transitions, the remaining discussion is limited to the case of CPPM's in a single-component plasma. Previous Raman[21] and neturon-scattering studies[22] of the dispersion properties of CPPM's in n-type zinc-blende semiconductors have revealed a CPPM with energy between the LO- and TO-phonon energies at wave vectors $>1\times10^{6}$ cm^{-1}. In the

case of the neutron-scattering experiment, the results were interpreted using a static screening argument in which, by definition, coupling effects involving plasmons are not included. In this model, the energy of the phonon-like ω_- mode is slightly below the TO-phonon energy at small wave vector because of the strong plasma screening. At larger wave vectors, it monotonically increases toward the LO-phonon energy as the screening power gradually decreases. In the case of the Raman experiments, the CPPM's spectra at different wave vectors were fit using the single-component plasma version of the theory described in Sec. III. While the significance of the Lindhard-Mermin form of the dielectric function was emphasized, no discussion on the physical mechanism responsible for the observation of CPPM energies between the LO- and TO-phonon energies was given.

CPPM's with energy intermediate to the LO- and TO-phonon energies have also been calculated[6,18] using a simplified, zero-wave-vector limit of the theory described in Sec. III. In these cases, the occurrence of such modes was attributed to the large phenomenological damping parameter used to generate the spectra, although the basic physical mechanism was not elaborated.

While none of these previous works reported a systematic study of the density dependence of their CPPM's, the observation of modes with energy intermediate to the LO- and TO-phonon energies suggests that they might have something in common with the CPPM's observed in p-type GaAs. If this is true, can the observed density dependence in p-type GaAs be explained in terms of static screening effects, effects due to large phenomenological damping, or to a combination of both? The remainder of this paper is devoted to answering this question. As part of the answer, heuristic physical models are developed that elucidate the nature of the physical phenomena that can in general lead to "anomalous" CPPM behavior.

First, consider the case of large wave vectors. A single-component plasma model, in which no phenomenological damping is included, can in fact produce a similar density dependence as observed in p-type GaAs, and the results can be understood in terms of the static screening picture described by Cowley and Dowling.[22] To see this, consider the behavior of the Lindhard-Mermin dielectric function in the limit of no phenomenological damping and large wave vector. For frequencies near those of the LO and TO phonons there is a wave vector above which the dimensionless η parameter in Eq. (6) is always $\ll 1$, and in this range the electronic part of the dielectric function will always be of the Debye-Hückel form. No plasmon–LO-phonon "coupling" can occur in this system because at densities such that the formal plasmon energy,

$$\omega_p = \left[\frac{4\pi N_{\rm fc} e^2}{m^*_{\rm fc} \epsilon_\infty} \right]^{1/2},$$

is comparable to the phonon energies, no plasmon resonance exists at these large wave vectors since there are insufficient carriers to screen or establish electric fields over a single wavelength of the (assumed) excitation. In this limit then, the equation used by Cowley and Dowling[22] to define the phonon energy, as screened by the free carriers, is strictly valid:

$$\omega(q)^2 = \omega_t^2 + (\omega_l^2 - \omega_t^2)/\epsilon(q,0) \tag{12}$$

and the corresponding density dependence shown in Fig. 6(a) follows immediately. Regardless of carrier density, the thermal velocity of the carriers is sufficient to adiabatically follow the ionic motion associated with the LO phonon. The free-carrier density is then always 180° out of phase with the ionic, bound charge density, but the ratio of magnitudes of the free-charge–to–bound-charge densities does depend on free-carrier density. At low densities it is essentially zero and the energy of the LO phonon is unperturbed. As the free-carrier density increases, the ratio increases and the macroscopic electric field responsible for raising the LO-phonon energy above the TO-phonon energy is gradually screened until at very high densities, it is completely screened (ratio $=-1$) rendering the LO phonon degenerate with the TO phonon.

A density-dependent CPPM energy similar to that observed for the p-type GaAs CPPM's can also be generated using a single-component plasma model at zero wave

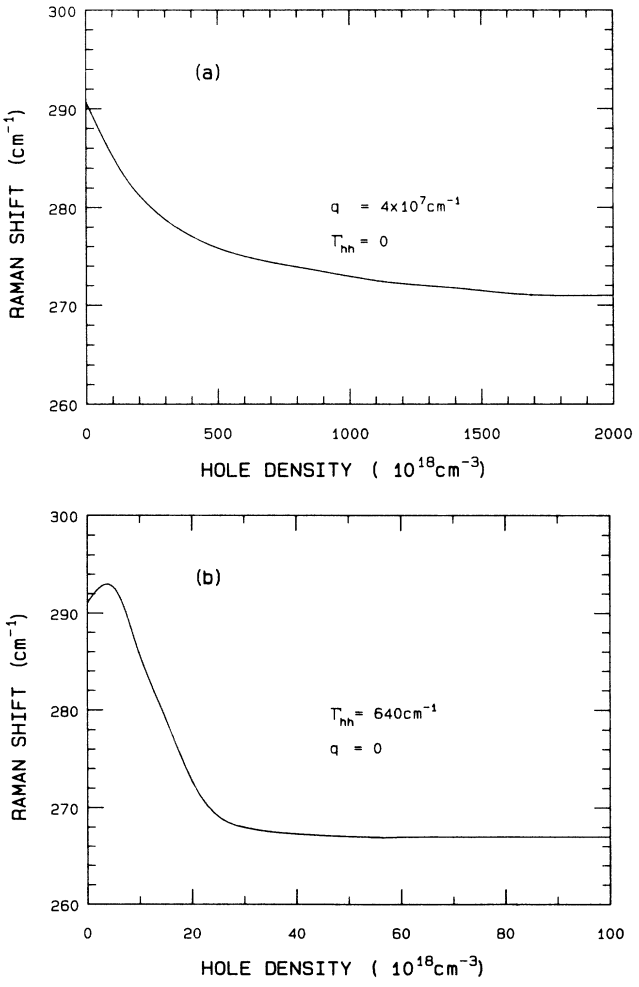

FIG. 6. The density-dependent energy(s) of the Raman peaks calculated with $\chi_{\rm fc}=\chi_{\rm hh}$ and (a) $q=4\times10^7$ cm^{-1}, $\Gamma_{\rm hh}=0$, or (b) $\Gamma_{\rm hh}=640$ cm^{-1}, $q=0$.

vector, and large phenomenological damping. In the small-wave vector limit, the Lindhard-Mermin susceptibility reduces to

$$\chi_{\rm fc}(q,\omega)=-\frac{\epsilon_\infty}{4\pi}\frac{\omega_p^2}{\omega(\omega+i\Gamma)}\left[1+\frac{3k_BT}{m^*_{\rm fc}}\frac{q^2}{(\omega+i\Gamma)^2}\right], \tag{13}$$

which is just the simple Drude result. In the limit that Γ is much larger than the phonon energies, the equation for the CPPM energies obtained by setting $\epsilon=0$ has one physically acceptable solution for free-carrier densities such that $\omega_p \leq \Gamma$. The situation is similar to the statically screened case described earlier in that there is no plasmon–LO-phonon "coupling" since no plasmon resonance exists. In this case the resonance is damped out of existence, whereas in the previous case it was a consequence of the excitation wavelength being less than the characteristic screening wavelength of the plasma. The single root $\epsilon=0$ thus corresponds again to the energy of the LO phonon as modified by the (nonresonant) free carriers. In the case of large damping, the resulting carrier density dependence, shown in Fig. 6(b), can be best understood by considering the expression for the ratio of free-charge–to–bound-charge-density amplitudes at the CPPM energy $\omega_{\rm pole}$,

$$\frac{\rho_f^{\rm pole}}{\rho_b^{\rm pole}}=\omega_p^2\frac{\omega_{\rm pole}^2-\omega_p^2-i\Gamma\omega_{\rm pole}}{(\omega_{\rm pole}^2-\omega_p^2)^2+\Gamma^2\omega_{\rm pole}^2}\ . \tag{14}$$

With reference to Fig. 7 and Eq. (14), at low carrier densities the vast majority of the free charge is 90° out of phase with the bound ionic charge. Since this free charge neither screens nor antiscreens the LO phonon its energy is shifted only a little. What remnant of the plasmon that does exist at low densities still has a natural frequency less than that of the LO phonon, so there is a very small amount of free charge that antiscreens the LO phonon, raising its energy *slightly*. Although negative, the magnitude of the in-phase component of the free-to-bound charge ratio is still very small because the large damping forces the majority of charge to be 90° out of phase. As the carrier density increases while the LO-phonon energy remains essentially unchanged, the plasma frequency rises above the LO-phonon energy, at which point the small resonant component of the free charge begins to screen rather than antiscreen the ionic charge. Thus for a free-carrier density such that the real part of the ratio in Eq. (14) changes sign, the energy of the CPPM dips slightly below the unscreened LO-phonon energy due to this small amount of screening, while the majority of the plasma is still 90° out of phase. As the free-carrier density continues to increase, but still with $\omega_p<\Gamma$, the plasma becomes more resonant in nature (though still overdamped), and an increasing number of carriers shift from being 90° out of phase to 180° out of phase, thus pulling the CPPM's energy lower and lower. Very close to the point where $\omega_p=\Gamma$, the real part of the ratio of free-to-bound charge in Eq. (14) becomes -1, and the CPPM has the TO-phonon energy, although there is still a significant amount of charge 90° out of phase. For higher densities the plasmon becomes a resonant entity and two CPPM's evolve in a fashion similar to that typically observed in *n*-type materials.

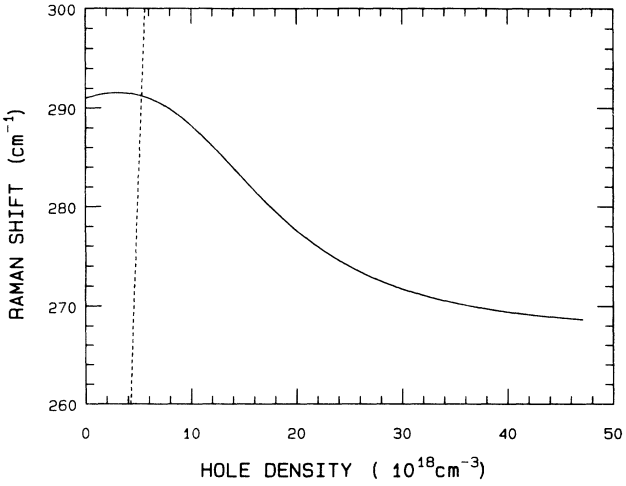

FIG. 7. The single-mode energy $\omega_{\rm pole}$ obtained by solving for $\epsilon=0$ with $\chi_{\rm fc}(q,\omega)=\chi_{\rm hh}(0,\omega)$ and $\Gamma_{\rm hh}=1000$ cm^{-1} (solid). Also shown is the density-dependent plasma frequency ω_p for comparison with Eq. 14 (dashed).

Thus it is possible to generate the observed density dependence of the *p*-type GaAs CPPM's through two completely different mechanisms. Since our full numerical fits to the spectra included both nonzero wave vector and phenomenological damping, these do not allow us to attribute the observed behavior to either of the two mechanisms. However, using a conservative criterion for the static screening model to hold for the heavy holes in GaAs, namely,

$$\left[\frac{m^*_{\rm fc}}{2k_BT}\right]^{1/2}\frac{\omega_l}{q}\sim 0.1\ , \tag{15}$$

the wave vector would have to be larger than $\sim 4\times10^7$ cm^{-1}. On the other hand, for the phenomenological damping mechanism to dominate, $\Gamma_{\rm hh}$ must be much greater than ω_l, which is definitely the case since $\Gamma_{\rm hh}=640$ cm^{-1} was used to obtain the fits to the spectra. Therefore we conclude that the observed density dependence of the CPPM's in *p*-type GaAs *largely* reflects the highly overdamped nature of the heavy holes in this material. However, as shown in Sec. IV, the light holes and the inter-valence-band transitions strongly modify the detailed density dependence of the CPPM's in *p*-type GaAs. The relatively slightly damped light holes act to reduce the overall damping in the system while the inter-valence-band transitions provide an additional intrinsic (as opposed to phenomenological) damping mechanism.

These arguments, together with the experimental results on Be-doped, *p*-type GaAs, illustrate that single-mode-like behavior with CPPM energies between those of the LO and TO phonons can in general be due to either static screening effects, effects due to the overdamped nature of the plasma, or to a combination of these two distinct physical mechanisms. Furthermore, the source of

the damping need not be extrinsic to the plasma system (that is, impurity or phonon induced). It can arise from intrinsic electronic processes such as inter-valence-band transitions (as in the *p*-type GaAs case), or intraband Landau damping processes, if these are not dominated by extrinsic effects.

VI. CONCLUSIONS

A systematic density dependent study of the influence of free holes on the LO-phonon mode in Be-doped, *p*-type GaAs grown by MBE was carried out using nonresonant Raman scattering. By quantitatively fitting the spectra with a multicomponent plasma model, intra-light-hole and inter-heavy- to light-hole transitions were found to contribute strongly to the LO-phonon–free-hole interaction. The novel single-mode behavior as a function of free-hole density was attributed largely to the overdamped nature of the heavy-hole system, although it was shown that wave-vector dispersion effects can in principle lead to the same density-dependent mode energy in systems with little or no damping.

ACKNOWLEDGMENTS

We would like to gratefully acknowledge the strong technical support of B. Kettles of N.R.C., and Dr. A. J. SpringThorpe and Dr. C. Miner of Bell Northern Research Ltd. for supplying some of the samples.

[1]B. B. Varga, Phys. Rev. **137**, A1896 (1985).
[2]A. Mooradian, in *Laser Handbook,* edited by F. T. Arecchi and E. O. Schultz-Dubois (Elsevier, New York, 1972).
[3]M. V. Klein, in *Light Scattering in Solids I,* edited by M. Cardona (Springer-Verlag, New York, 1983).
[4]G. Abstreiter, in *Light Scattering in Solids IV,* edited by M. Cardona (Springer-Verlag, New York, 1984).
[5]H. R. Chandrasekhor and A. K. Ramdas, Phys. Rev. B **21**, 1511 (1980).
[6]D. T. Hon and W. L. Faust, Appl. Phys. **1**, 241 (1973).
[7]D. Olego and M. Cardona, Phys. Rev. B **24**, 7217 (1981).
[8]T. Kamijoh, A. Hashimoto, H. Takano, and M. Sakuta, J. Appl. Phys. **59**, 2382 (1986).
[9]Tonao Yuasa and Makoto Ishii, Phys. Rev. B **35**, 3962 (1987).
[10]S. Buchner and E. Burstein, Phys. Rev. Lett. **33**, 908 (1974).
[11]M. Klein, B. N. Ganguly, and P. J. Colwell, Phys. Rev. B **6**, 2380 (1972).
[12]N. D. Mermin, Phys. Rev. B **1**, 2362 (1970); P. M. Platzman and P. A. Wolff, in *Waves and Interactions in Solid State Plasmas,* edited by H. Ehrenreich, F. Seitz, and D. Turnbull (Academic, New York, 1973), p. 62.
[13]W. Bardyszewski, Solid State Commun. **57**, 873 (1986).
[14]J. Monecke, Phys. Status Solidi B **121**, 329 (1984).
[15]The slight differences between the estimated hole concentrations listed in Table I and those in our previous paper, Ref. 16, are due to the wave-vector dependence of the intra-light-hole transitions, which was incorrectly taken to be of the Drude form [small-q limit of the correct form in Eq. (6)].
[16]Kam Wan, Jeff F. Young, R. L. S. Devine, W. T. Moore, A. J. SpringThorpe, C. J. Miner, and P. Mandeville, J. Appl. Phys. **63**, 5598 (1988).
[17]H. J. Lee and D. C. Look, J. Appl. Phys. **54**, 4446 (1983).
[18]G. Irmer, V. V. Toporov, B. H. Batramov, and J. Monecke, Phys. Status Solidi B **119**, 595 (1983).
[19]Heinz Nather and Lucia G. Quagliano, J. Lumin. **30**, 50 (1985).
[20]A. Pinczuk, J. Shah, and P. A. Wolff, Phys. Rev. Lett. **47**, 1487 (1981).
[21]G. Abstreiter, R. Trommer, M. Cardona, and A. Pinczuk, Solid State Commun. **30**, 703 (1979).
[22]R. A. Cowley and G. Dolling, Phys. Rev. Lett. **14**, 549 (1965).